Are Time-Dependent Fluorescence Shifts at the Tunnel Mouth of Haloalkane Dehalogenase Enzymes Dependent on the Choice of the Chromophore?

Mariana Amaro,[†] Jan Brezovský,[‡] Silvia Kováčová,[§,||] Lukáš Maier,[§,||] Radka Chaloupková,*,[‡] Jan Sýkora,*,[†] Kamil Paruch,*,[§,||] Jiří Damborský,[‡,§] and Martin Hof[†]

[†]J. Heyrovsky Institute of Physical Chemistry of the ASCR, v. v. i., Academy of Sciences of the Czech Republic, Dolejskova 3, 182 23 Praha, Czech Republic

[‡]Loschmidt Laboratories, Department of Experimental Biology and Research Centre for Toxic Compounds in the Environment, Faculty of Science, Masaryk University, Kamenice 5/A13, 625 00 Brno, Czech Republic

[§]International Centre for Clinical Research, St. Anne's University Hospital Brno, Pekarska 53, 656 91 Brno, Czech Republic

[||]Department of Chemistry, Faculty of Science, Masaryk University, Kamenice 5/A8, 625 00 Brno, Czech Republic

S *Supporting Information*

ABSTRACT: Time-dependent fluorescence shifts (TDFS) of chromophores selectively attached to proteins may give information on the dynamics of the probed protein moieties and their degree of hydration. Previously, we demonstrated that a coumarin dye selectively labeling the tunnel mouth of different haloalkane dehalogenases (HLDs) can distinguish between different widths of tunnel mouth openings. In order to generalize those findings analogous experiments were performed using a different chromophore probing the same region of these enzymes. To this end we synthesized and characterized three new fluorescent probes derived from dimethylaminonaphthalene bearing a linker almost identical to that of the coumarin dye used in our previous study. Labeling efficiencies, acrylamide quenching, fluorescence anisotropies, and TDFS for the examined fluorescent substrates confirm the picture gained from the coumarin studies: the different tunnel mouth opening, predicted by crystal structures, is reflected in the hydration and tunnel mouth dynamics of the investigated HLDs. Comparison of the TDFS reported by the coumarin dye with those obtained with the new dimethylaminonaphthalene dyes shows that the choice of chromophore may strongly influence the recorded TDFS characteristics. The intrinsic design of our labeling strategy and the variation of the linker length ensure that both dyes probe the identical enzyme region; moreover, the covalently fixed position of the chromophore does not allow for a major relocalization within the HLD structures. Our study shows, for the first time, that TDFS may strongly depend on the choice of the chromophore, even though the identical region of a protein is explored.
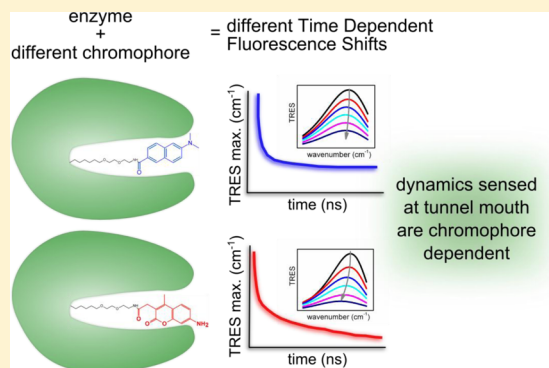
INTRODUCTION

The relation between the catalytic activity and dynamics of protein moieties and their degree of hydration involved in enzymatic reactions is of significant interest.[1−5] One of the methods suitable for monitoring the hydration and mobility of a particular protein region is "time-dependent fluorescence shift" (TDFS), which has been used widespread in the recent years.[6−10] The method takes advantage of a rapid change of the fluorophore dipole moment upon electronic photoexcitation. The surrounding solvent dipoles, still arranged according to the initial ground state charge distribution of the fluorophore, start to reorientate to re-establish an equilibrium.[11] As a result, time-resolved emission spectra (TRES) emitted continuously throughout this relaxation process are red shifted.[12] The time window accessible for capturing the shift is determined on one

side by the temporal instrument resolution and on the other side by the lifetime of the fluorophore.[13] Analysis of the magnitude and kinetics of the TDFS reports on the polarity and mobility of the fluorophore's microenvironment, respectively. Recent contributions[14−17] initiated the debate on to what extent the motions of the water molecules and protein fluctuations contribute to the recorded TDFS and how these motions are coupled together. Both experimental and theoretical approaches reach the agreement that the water and protein motions are strongly correlated on time scales longer than tens of picoseconds, and consequently, TDFS

reports on the local structural properties of the protein on these longer time scales.[14,15] TDFS emphasize the dynamic aspects of the proteins in solution serving as an extremely useful complementary tool to the "static" structural approaches, such as X-ray diffraction.

To guarantee the validity of TDFS measurements in proteins the probe has to emit exclusively from the position of interest within the protein matrix. Several approaches have been developed to reach such selectivity utilizing natural fluorophores like tryptophans,[18−20] flavins,[21] and hemes[22] or labeling the proteins via their SH and NH₂ groups.[23−26] An alternative labeling method[27] has been used in our recent contribution investigating haloalkane dehalogenases (HLDs).[10] Briefly, the dye is designed to contain a fluorophore (in our case Coumarin-120) and a linker with the Cl atom attached at the end (Figure 1).
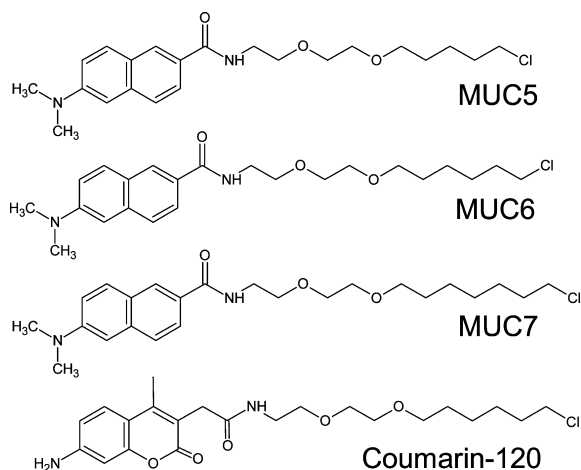

Figure 1. Structures of the fluorescent dyes used in this article. Three top structures depict variants of MUC dye differing in linker length. Structure of Coumarin-120, which was used in the previous study,[10] is shown at the bottom.

The dehalogenase binds the dye as a substrate; however, a single point mutation in the active site of HLD prevents hydrolysis of the covalent enzyme−substrate intermediate.[27] As a result, the complex of the dehalogenase with the covalently bound dye is preserved. By means of this approach we characterized the TDFS in the biologically relevant part of dehalogenases,[10] namely, their tunnel mouths. This particular enzyme region is evolutionarily the most variable one in the structure of HLDs originating from different bacterial species and believed to have an impact on the enzymatic reaction.[28] Specifically, it has been shown that access tunnel arrangements determine kinetics,[29] selectivity,[30] reaction mechanism,[31] and stability of enzymes.[32] We investigated two HLDs, DhaA from *Rhodococcus rhodochrous* NCIMB13064[33] and DbjA from *Bradyrhizobium japonicum* USDA110,[34] possessing different enzyme activity as well as different tunnel architecture. Indeed, the TDFS response was found to be enzyme dependent. DhaA, for which the X-ray diffraction reveals a narrower tunnel mouth, exhibited slower TDFS kinetics when compared to DbjA. This indicates a lower mobility probed in DhaA's tunnel mouth supporting the diffraction data. Moreover, the overall TDFS in the DbjA enzyme was larger than that observed for DhaA, pointing to higher polarity/hydration within this protein region.

In this contribution a fundamental question for the use of TDFS not only in proteins but also in other supramolecular assemblies is addressed: Is the recorded TDFS response in proteins affected by the chemical nature of the probe? A main requirement for answering that question is that the chromophores to be compared must locate indeed selectively at identical sites within the examined supramolecular assembly. Thus, strategies based on noncovalent labeling often used in proteins,[25] micelles,[35,36] or lipid vesicles[37] appear to be less suitable.

We synthesized a compound containing a dimethylaminonaphthalene chromophore and a linker identical to that of the Coumarin-120 dye used in our previous study.[10] The newly synthesized probe was named MUC7, and its structure is depicted in Figure 1. Moreover, we synthesized analogues of MUC7 having different linker lengths (MUC6 and MUC5 shortened by 1 and 2 carbon atoms, respectively) with the intent to map differences in hydration and mobility along the tunnel mouth. With these newly synthesized dyes in hand we were able to monitor the identical region of the HLD mutants DbjA and DhaA previously characterized by Coumarin-120. Comparison of these results verifies the conclusions drawn from the Coumarin-120 experiments and shows that the TDFS may quantitatively differ from chromophore to chromophore. In the first part of this article we focus on characterization of the newly synthesized probes in solvents and model systems to prove their suitability for TDFS studies. Docusate sodium (AOT) reverse micelles[38] serve ideally for this purpose since the amount of water molecules confined by the detergent's polar heads can be tuned in a defined manner to create an environment that mimics the protein−water interface to a large extent.[39] In the latter part of the article the results gained with the set of MUC probes for the two HLDs, DbjA and DhaA, are discussed and compared to those obtained with Coumarin-120.

■ EXPERIMENTAL SECTION

Synthesis of MUC Dyes. Description of the synthesis and related NMR spectra are given in the Supporting Information.

Construction of DhaA and DbjA Variants Carrying Mutation in the Catalytic Histidine. Mutant recombinant genes were obtained using a QuikChange Site-Directed Mutagenesis Kit (Stratagene, La Jolla, CA) according to the manufacturer's instructions. Specific complementary primers (5′-CATCGGCCCGGGATTG**TT**CTACCTCCAGGAAG-3′ and 5′-CTCGGCGCGGG ATTG**TT**CTATCTGCAGGAGG-3′) carrying substitution (in bold) were designed for mutagenesis of *dhaA* and *dbjA* recombinant genes, respectively. Plasmids pUC18-*dhaA* and pUC18-*dbjA* containing sequence encoding for the histidine tail on the C terminus of the resulting protein were used as templates. Mutant recombinant genes *dhaA* and *dbjA* were subcloned into expression vector pAQN[40] using *Bam*HI and *Hin*dIII restriction sites.

Expression of DbjA-H280F and DhaA-H272F in *Escherichia coli* and Purification. After verification of the sequence by DNA sequencing, the plasmid was transformed into *E. coli* BL21 for protein expression. For overexpression, cells were grown at 37 °C to an optical density about 0.6 at 600 nm in Luria−Bertani (LB) medium (Sigma-Aldrich, St. Louis, MO) with ampicillin (100 μg/mL). Protein expression was induced by adding isopropyl β-D-1-thiogalactopyranoside to a final concentration of 0.5 mM in LB medium. The temperature was decreased to 30 °C. Cells were harvested by 12 min centrifugation at 3700g after 4 h of cultivation, washed by 20

mM potassium phosphate buffer with 10% glycerol (pH 7.5), and then resuspended in the same buffer. Harvested cells were stored at −80 °C overnight. Defrosted culture was disrupted by sonication with Soniprep 150 (Sanyo Gallenkamp, Loughborough, U.K.), and the lysate was centrifuged at 21 000g for 1 h. The crude extract was applied on a nickel–nitrilotriacetic acid (Ni-NTA) Superflow column (QIAGEN, Hilden, Germany) equilibrated with purification buffer of pH 7.5 composed of 16.4 mM K_2HPO_4, 3.6 mM KH_2PO_4, and 0.5 M NaCl containing 10 mM imidazole. Unbound and weakly bound fractions were eluted with purification buffer with 50 mM imidazole. Histidine-tagged protein was eluted with purification buffer with 300 mM imidazole. The eluted protein was dialyzed against 50 mM phosphate buffer composed of 41 mM K_2HPO_4 and 9 mM KH_2PO_4 (pH 7.5). Protein concentration was determined by the method of Bradford (Sigma-Aldrich, St. Louis, MO). Protein purity and size was verified by sodium dodecyl sulfate–polyacrylamide gel electrophoresis (SDS-PAGE).

Labeling of DbjA-H280F and DhaA-H272F by Coumarin and MUC Dyes. Proteins DbjA-H280F and DhaA-H272F were diluted to a final concentration of 50 μM by 50 mM phosphate buffer (pH 7.5). HaloTag Coumarin-120 Ligand (Promega Corporation, Madison, WI) was added to the enzyme solution to a final concentration 15 μM. The solution was incubated for 15 min at 37 °C and loaded on a 1 mL Ni-NTA HisTrap HP column (Amersham Biosciences, Freiburg, Germany) pre-equilibrated with buffer composed of 16.4 mM K_2HPO_4, 3.6 mM KH_2PO_4, and 0.5 M NaCl containing 10 mM imidazole (pH 7.5). Unbound ligand was washed out by 100 mL of buffer used for pre-equilibration of the column. The same procedure was applied for the MUC dyes. The protein–dye complex was eluted from the column by buffer containing 300 mM imidazole. Protein–dye sample was then dialyzed against 20 mM glycine buffer (pH 8.2) to remove imidazole and NaCl and immediately used for fluorescence measurements.

Preparation of Docusate Sodium (AOT) Reverse Micelles. AOT reverse micelles were prepared according to Chattopadhyay et al.[41] Briefly, 50 mM solution of AOT in heptane was added to a test tube covered with a dried film of the fluorescence probe. Sample was gently heated up to 35 °C for 1 h and vortexed every 10 min to enable probe incorporation. The final ratio of fluorophore:surfactant was chosen to be 1:6000. Therefore, each reverse micelle is likely to contain one dye molecule at most. Proper aliquots of water were then added to achieve the desired values of water–surfactant molar ratio (w_0).

Steady-State and Time-Resolved Fluorescence Measurement. Steady-state excitation and emission spectra were recorded on a Fluorolog-3 spectrofluorometer (model FL3-11; HORIBA Jobin Yvon Inc., Edison, NJ) equipped with a Xenon arc lamp. All spectra were collected in 1 nm steps (2 nm bandwidths were chosen for both the excitation and the emission monochromators). The temperature in the cuvette holder was maintained within ±0.1 °C using a water-circulating bath at 10 and 45 °C. When performing fluorescence quenching measurements samples were excited at 350 nm and emission detected at 440 nm.

Steady-state anisotropy was measured at the same wavelength regions as the quenching experiments with polarizers inserted into the setup. Four intensities of polarized fluorescence (I_{VV}, I_{VH}, I_{HV}, I_{HH}) were recorded, where "V"

and "H" in the subscripts stand for the vertical and horizontal directions and the first and second subscript denote the direction plane of the polarization in the excitation and emission arm, respectively. Steady-state anisotropy is calculated as follows

$$r_{st} = \frac{I_{VV} - GI_{VH}}{I_{VV} + 2GI_{VH}} \tag{1}$$

in which G is the instrumental correction factor given by the observed ratio, I_{HV}/I_{HH}. Absorption spectra were recorded on a Perkin-Elmer Lambda 19 spectrometer (Perkin-Elmer, Wellesley, MA).

Fluorescence decays were collected by using a IBH 5000 U SPC (HORIBA Jobin Yvon Inc., Edison, NJ) with a picosecond diode laser (IBH NanoLED 11, 370 nm peak wavelength, 0.1 ns pulse width, 1 MHz repetition rate) and a cooled Hamamatsu R3809U-50 microchannel plate photomultiplier (Hamamatsu, Shizuoka, Japan) with 40 ps time resolution. Emission decays were recorded at a series of wavelengths spanning the steady-state emission spectrum (400−490 nm) in 10 nm steps. In order to eliminate scattered light, a 399 nm cutoff filter was used. The signal was kept below 2% of the light source repetition rate, and data were collected in 4096 channels (0.028 ns per channel) until the peak value reached 5000 counts. Fluorescence decays were fitted to multiexponential functions using the iterative reconvolution procedure with IBH DAS6 software.

Time-resolved emission spectra (TRES) were obtained by the spectral reconstruction method as described before.[12] In order to determine the position of the spectra ν (i.e., their maxima) and their full widths at half-maximum (fwhm), TRES were fitted by a log-normal function. The time evolution of the TRES maximum $\nu(t)$ was treated with the multiexponential function

$$\nu(t) = \nu(\infty) + (\nu(0) - \nu(\infty)) \sum_i a_i \exp(-t/\tau_i) \tag{2}$$

where $\nu(0)$ and $\nu(\infty)$ are the emission maxima at time zero (further discussed in this paper) and at time infinity (gained by extrapolation of $\nu(t)$), respectively. a_i corresponds to the contribution of the particular relaxation time τ_i to $\nu(t)$. In Table 3, $\%A_i$ is equal to $100a_i$ and % obs is the portion of TDFS occurring at times longer than the instrumental temporal resolution (~40 ps) expressed in percent.

The correlation function $C(t)$ was calculated from the emission maxima $\nu(t)$ of the TRES at time t after excitation according to

$$C(t) = \frac{\nu(t) - \nu(\infty)}{\nu(0) - \nu(\infty)} \tag{3}$$

To characterize the overall time scale of solvent response an average relaxation time was calculated as follows

$$\tau_r = \int_0^\infty C(t)dt \tag{4}$$

RESULTS AND DISCUSSION

Photophysical Behavior of the Newly Synthesized MUC Dyes and TDFS in Confined Water Systems: Comparison with the Coumarin-120 Analogue. To characterize the basic photophysical properties of MUC7, absorption and emission spectra were recorded in a set of

solvents of various polarities. As obvious from Table S1, Supporting Information, an increase in the solvent polarity leads to a red shift in both the absorption and the emission maxima. More importantly, the overall Stokes shift $\Delta\nu_{AE}$ shows a linear dependence (Figure 2) on solvent polarity, which
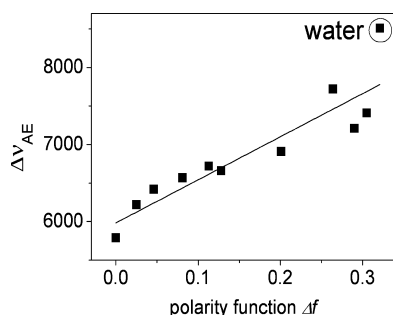

Figure 2. Dependence of MUC7 Stokes shift, $\Delta\nu_{AE}$, on solvent polarity. Line represents a linear fit. Value obtained for water is highlighted since it shows deviation from linearity due to specific interactions.

indicates the suitability of the MUC dye for recording TDFS. Nevertheless, an additional shift on the order of 600 cm^{-1} occurs for $\Delta\nu_{AE}$ in water, indicating a minor effect of specific interactions in this solvent. Since the TDFS in the herein investigated proteins is mainly occurring on the nanosecond time scale,[10] we decided to map and compare the TDFS of the MUC dyes and Coumarin-120 in glycerol and AOT reverse micelles (Table 1). In the high-viscous solvent, the MUC probe

Table 1. Parameters Gained by Recording Time Resolved Fluorescence and TDFS for MUC7 and Coumarin-120 in Glycerol (23 °C) and AOT Reverse Micelles (10 °C)[a]

probe, system	τ_{av} (ns)	$\Delta\nu$ (cm^{-1})	ν_0 (cm^{-1})	τ_{SR} (ns)	% obs
MUC7, glycerol	5.10	2040	24 100	1.0	59
Coumarin-120, glycerol	3.81	1660	23 800	0.9	69
MUC7, AOT, $w_0 = 1$	6.83	1800	25 430	10.0	86
MUC7, AOT, $w_0 = 2$	6.32	2270	25 150	6.2	92
MUC7, AOT, $w_0 = 5$	5.85	2860	25 120	2.0	73
Coumarin-120, AOT, $w_0 = 1$	3.82	1650	23 310	12.9	109
Coumarin-120, AOT, $w_0 = 2$	4.03	1160	23 310	3.1	77
Coumarin-120, AOT, $w_0 = 5$	4.08	1370	23 410	0.4	35

[a] τ_{av} is the average fluorescence lifetime recorded at 420 nm, $\Delta\nu$ stands for the overall value of TDFS, ν_0 represents the maximum of the spectrum obtained by "time 0 estimation" as described in the supplement, τ_{SR} is the relaxation time, and % obs corresponds to the portion of the TDFS occurring on the time scale slower than the temporal experimental resolution of 40 ps (expressed in percents). Detailed description of the parameters can be found in the Experimental Section.

possesses a higher lifetime and larger magnitude of TDFS compared to Coumarin-120. On the other hand, TDFS kinetics occurs on the analogous time scale as illustrated by the comparable values of relaxation time τ_{SR} and the observed portion of TDFS. Such behavior is anticipated as the TDFS kinetics reflects the microviscosity of the probe environment being identical for both dyes in glycerol. A different picture is observed when inspecting AOT reverse micelles. In this model

system the water:surfactant molar ratio (expressed as w_0) determines the size of these nanoaggregates, which contain a limited number of water molecules surrounded by polar head groups of detergent.[39,42] Water confined in such a way exhibits significantly different properties from bulk. At w_0 lower than 2, water molecules are strongly associated to the polar heads of surfactant and thus slow down the relaxation dynamics to the nanosecond time scale. At w_0 higher than 2, a water pool is formed accelerating the relaxation dynamics.[43] The results obtained with MUC7 and Coumarin-120 are shown in Figure 3 and Table 1. Data presented for both dyes illustrates that MUC7 is a more appropriate candidate for TDFS studies.
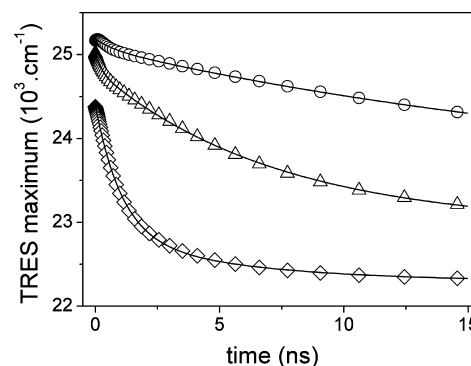

Figure 3. Time evolution of TRES maxima obtained for MUC7 in AOT micelles for $w_0 = 1$ (circles), $w_0 = 2$ (triangles), and $w_0 = 5$ (squares). Solid lines represent 3-exponential decay fits.

First, its fluorescence lifetime τ_{av} is longer compared to Coumarin-120s, enabling one to monitor slower TDFS kinetics. Furthermore, its overall dynamic Stokes shift $\Delta\nu$ is considerably larger, yielding 2900 cm^{-1} in reverse micelles at $w_0 = 5$ whereas $\Delta\nu$ measured for Coumarin-120 in bulk water was estimated to reach only 1700 cm^{-1} (data not shown). Finally, the photophysics of Coumarin-120 is more complex since additional intramolecular relaxation[44] interferes in nonpolar environments. As a result, the recorded $\Delta\nu$ reported by Coumarin-120 at the lowest w_0 values is anomalously large, being even larger than the values for the fully hydrated system at $w_0 \approx 5$ (Table 1). In contrast, the data gained with the MUC7 probe do not show any deviation from the anticipated trends, i.e., the relaxation dynamics reflected by τ_{SR} is accelerated as well as $\Delta\nu$ is increased at higher water content. On the basis of these facts, we can conclude that the newly designed probe is suitable for monitoring TDFS. Moreover, it surpasses the probe based on Coumarin-120 in many respects, e.g., longer lifetime, higher Stokes shifts, and simpler photophysics.

A direct comparison of reported TDFS kinetics indicates an elevated water solubility of the Coumarin-120 chromophore compared to the MUC one: while at very low water content both dyes report practically identical TDFS kinetics, addition of water accelerates the TDFS reported by Coumarin-120 much more effectively than in the case of MUC7. In the fully hydrated system ($w_0 \approx 5$) two-thirds of the TDFS reported by Coumarin-120 occurs on a time scale faster that the resolution of our experiment (40 ps), while in the same system MUC7's shift is predominately a nanosecond process. Vincent et al. showed that the fluorophore's linker affects the position of the dye inside the AOT micelles which influences the TDFS response due to the different probed ratios of interfacial/bulk

water.[39] However, in our study we focus on the influence of the chromophore. Even though both compounds bear the identical aliphatic linker, at high water contents, the Coumarin-120 (dipole moment $\mu \approx 5.26$ D) dye apparently relocates toward the created water pool while the MUC7 ($\mu \approx 1.25$ D) remains located at the detergent's polar head groups due to some specific interaction.

Labeling of DbjA-H280F and DhaA-H272F by MUC Dyes. Proper incorporation of the MUC probes into HLDs DbjA-H280F and DhaA-H272F was tested by means of steady-state anisotropy and acrylamide quenching for all three MUC variants (Table 2, Figure 4). Obviously, the Stern–Volmer plot

Table 2. Characteristics of HLDs Variants, DbjA-H280F, and DhaA-H272F, Labeled with Coumarin-120, MUC6, and MUC7[a]

	τ_{av} (ns)	r_{st}	K_{SV} (M^{-1})	k_q (10^{-8} M^{-1} s^{-1})
Coumarin-120:DbjA-H280F	4.37	0.19	0.25	0.57
Coumarin-120:DhaA-H272F	3.93	0.25	0.12	0.31
MUC6:DbjA-H280F	6.47	0.18	0.45	0.70
MUC6:DhaA-H272F	7.42	0.22	0.35	0.47
MUC7:DbjA-H280F	6.64	0.17	0.46	0.69
MUC7:DhaA-H272F	7.80	0.22	0.37	0.48

[a]MUC5 is not included in the table since its labeling failed as shown from the Stern–Volmer plots. τ_{av} denotes the average lifetime, r_{st} stands for steady-state anisotropy, and K_{SV} and k_q represent the Stern–Volmer and quenching rate constants, respectively.
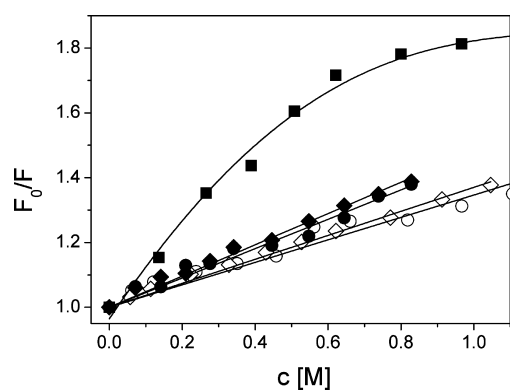

Figure 4. Stern–Volmer plots for MUC dyes bound to DbjA-H280F and DhaA-H272F. Solid symbols correspond to DbjA-H280F (squares, MUC5; circles, MUC6; diamonds, MUC7) and the open symbols to DhaA-H272F (circles, MUC6; diamonds, MUC7). All samples show a linear dependence on acrylamide concentration with the exception of the MUC5:DbjA-H280F complex.

obtained for the MUC5:DbjA-H280F complex is biphasic, showing the presence of more locations within the protein, thus indicating nonspecific binding. Additionally, the labeling efficiency for this dye was significantly lower compared to the other MUC variants. Incorporation into DhaA-H272F, which possesses a narrower tunnel mouth according to the crystal structure, was even completely unsuccessful. Seemingly, the linker is too short to reach the active site with the relatively bulky chromophore which hampers or blocks at some point the approach to the reaction center. Consequently, we did not use the MUC5 dye in the following TDFS studies.

The remaining variants MUC6 and MUC7 behave according to our expectations (Table 2). The Stern–Volmer plots remain linear for all investigated mutants (Figure 4), and the quenching constants k_q are on the same scale as for the HLDs labeled with Coumarin-120. The anisotropies of MUC6 and MUC7 are lower for DbjA-H280F (wider tunnel mouth determined from the crystal structure) than DhaA-H272F (narrower tunnel mouth determined from the crystal structure), which is again in agreement with the data obtained with Coumarin-120. Additionally, the higher values of steady-state anisotropy observed for the Coumarin-120 dye compared to the MUC dyes can be explained by the longer lifetimes of the newly synthesized MUC probes.

In conclusion, the HLDs specific labeling with MUC6 and MUC7 is successful, while the linker of MUC5 is too short, and an interaction between the bulky chromophore and the protein matrix at the tunnel hampers the access to the active site. Labeling efficiencies, acrylamide quenching, as well as fluorescence anisotropies for all 4 examined fluorescent MUC:HLD complexes confirm the picture gained from the crystal structures,[30,45] i.e., that the tunnel mouth of DbjA-H280F is broader compared to that of DhaA-H272F.

TDFS Monitored by MUC6 and MUC7 in DhaA-H272F. The results obtained in the solvents and AOT reversed micelles proved that the MUC dyes are suitable for monitoring TDFS. Moreover, their fluorescence characteristics are superior to the previously used dye Coumarin-120, i.e., longer lifetime and larger TDFS. Therefore, the MUC dyes might be expected to provide a more detailed view on the solvation response at the tunnel mouth of HLDs.

Before measuring the TDFS response in proteins the "time 0 spectrum" ($\nu(0)$),[46] i.e., the spectrum emitted prior to the solvent relaxation starting, was successfully estimated. We encountered the problem that the concentration of labeled protein was too low to allow measurements of the probe's absorption spectra. Nevertheless, we developed an alternative approach which has been successfully tested on AOT micelles. In this approach we make use of the excitation spectra measured at the very blue edge of MUC's emission. Method details are described in the Supporting Information.

TDFS results obtained for DhaA-H272F labeled with the MUC probes and Coumarin-120 are summarized in Table 3. On the basis of the measurements in AOT reverse micelles (Table 1) the magnitude of TDFS might be expected to reach significantly higher values for MUC6 and MUC7 when compared to Coumarin-120. However, we find it is increased only slightly from 950 cm^{-1} for Coumarin-120 to 1050 and 1140 cm^{-1} for MUC6 and MUC7, respectively. Curiously enough the TDFS kinetics recorded for the MUC probes exhibits even larger deviations from the one recorded for Coumarin-120. The overall relaxation time τ_{SR} is reduced by more than factor of 10 for the MUC dyes ($\tau_{SR} \approx 0.1$ and 0.4 ns for MUC6 and MUC7, respectively) compared to Coumarin-120 ($\tau_{SR} \approx 4.1$ ns) even though the fluorescence lifetime of MUC is significantly longer (Table 3). Additional fitting of the time evolution of TRES $\nu(t)$ revealed that in the case of MUC a nanosecond TDFS component (τ_3 in Table 3) is negligible for DhaA-H272F labeled with MUC6 at 10 °C, and for MUC7 the contribution of τ_3 was below 10% to the TDFS kinetics, Figure 5.

In order to elucidate such apparent inconsistency in TDFS kinetics recorded by MUC, we raised the temperature to 45 °C at which the protein conformation is still not significantly

Table 3. Parameters Gained by Analysis of TDFS Obtained for HLDs Mutants DbjA-H280F and DhaA-H272F Labeled with Coumarin-120, MUC6, and MUC7[a]

probe, system	$\Delta\nu$ (cm^{-1})	ν_0 (cm^{-1})	τ_{SR} (ns)	τ_1 (ns) (% A$_1$)	τ_2 (ns) (% A$_2$)	τ_3 (ns) (% A$_3$)	% obs
Coumarin-120:DhaA-H272F, 10 °C[b]	950	23 300	4.1	<0.03 (43)	1.3 (36)	12.6 (21)	90
Coumarin-120:DbjA-H280F, 10 °C[b]	1300	23 400	2.8	<0.03 (63)	1.4 (17)	11.0 (20)	70
MUC6:DhaA-H272F, 10 °C	1050	24 480	0.1	<0.03 (80)	0.73 (20)		20
MUC7:DhaA-H272F, 10 °C	1190	24 590	0.4	<0.03 (72)	0.36 (20)	3.3 (8)	29
MUC6:DhaA-H272F, 45 °C	1300	24 410	1.7	<0.03 (62)	0.60 (23)	22.2 (15)	37
MUC7:DhaA-H272F, 45 °C	1350	24 460	0.9	<0.03 (58)	0.20 (27)	5.1 (15)	42
MUC6:DbjA-H280F, 10 °C	1420	24 210	6.6	<0.03 (25)	0.3 (16)	14.9 (59)	75

[a]$\Delta\nu$ stands for the overall value of TDFS, ν_0 represents the maximum of the spectrum obtained by "time 0 estimation" as described in the supplement, τ_{SR} is the relaxation time, τ_i and A_i represent the output of the exponential fitting of TRES (TRES alone are depicted in Figure S1, Supporting Information) maxima $\nu(t)$ representing the characteristic times and amplitudes (in percent), respectively, and % obs corresponds to the portion of the TDFS occurring on the time scale slower than 40 ps (expressed in percent). Please note that the given value of the overall relaxation time τ_{SR} is misleading: at least in the systems where τ_{SR} values are smaller than 1 ns a large part of the reorientation of the dye environment is not complete during the fluorescence lifetime of the MUC dye. For explanation, see the text. [b]Data published in the previous contribution.[10]
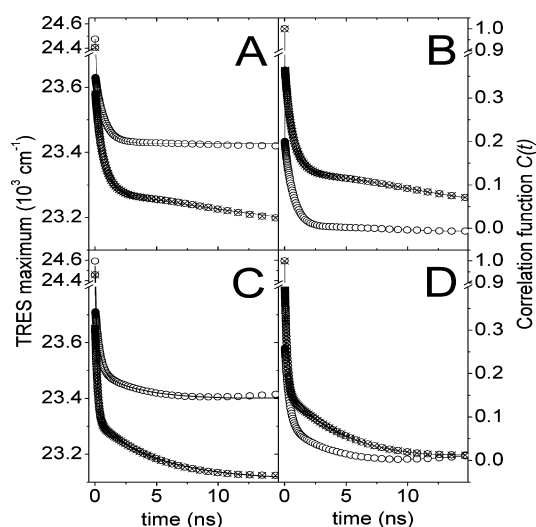

Figure 5. TDFS results obtained for DhaA-H272F labeled with MUC6 and MUC7 at two different temperatures. Open and crossed out symbols stand for experiments performed at temperatures of 10 and 45 °C, respectively. (A) Time course of MUC6:DhaA-H272F TRES maxima, (B − correlation function $C(t)$ for MUC6:DhaA-H272F, (C) time course of MUC7:DhaA-H272F TRES maxima, (D) correlation function for MUC7:DhaA-H272F.

impaired (Figure S3, Supporting Information). In this case the amplitude of the nanosecond component, τ_3, contributes to the data to a higher extent than at 10 °C and is also prolonged. Strikingly, the captured part of TDFS (parameter % obs, Table 3) grows significantly upon temperature increase and the overall relaxation time, τ_{SR}, also becomes higher, which is in contradiction to the entire literature of TDFS in proteins,[47−49] micelles,[50] or vesicles.[51] Moreover, a considerable increment of approximately 200 cm^{-1} in the overall Stokes shift was detected for both MUC6 and MUC7 at 45 °C compared to 10 °C. The only possible explanation for these findings is that a substantial part of the reorientation dynamic at 10 °C occurs on a time scale slower than MUC's nanosecond lifetime, therefore being beyond our experimental nanosecond time window. In other words, the TDFS of MUC6 and MUC7 at 10 °C does not reach its equilibrium level during the nanosecond lifetime of the probe. Increasing the temperature accelerates the "virtual" submicrosecond component to the nanosecond time scale, thus making the slower relaxation and protein reorganization process at least partially detectable by MUC's nanosecond

fluorescence. Our data shows that the close environment of MUC6 and MUC7 at the tunnel mouth of DhaA-H272F at 10 °C is characterized by motions occurring to a significant extent on a submicrosecond time scale.

Comparison with previously published data demonstrates that even though the identical covalent linker of MUC7 and Coumarin-120 ensures that both dyes are probing the identical region of the tunnel mouth, their recorded TDFS at 10 °C differ strongly. In the case of Coumarin-120 the slow part of reorientation kinetics present with the MUC dyes is missing and the TDFS reaches its equilibrium level during Coumarin-120s fluorescence decay. To explain such difference, we propose that a specific interaction between the MUC probe and the protein matrix is responsible for the submicrosecond kinetics. We speculate that the difference in the hydrophobicity and dipole moment of the MUC chromophore ($\mu \approx 1.25$ D) when compared to Coumarin-120 ($\mu \approx 5.26$ D) might give preference to a specific hydrophobic or electrostatic adhesion of the MUC chromophore to the protein matrix at the tunnel mouth. Alternatively, the steric effects may also cause different positioning of the investigated probes within the tunnel mouth, since Coumarin-120, in contrast to MUC dyes, bears two non-H substituents adjacent to the ring-tether linkage and there is a methylene group added in between the carbonyl group and aromatic moiety.

The slow component of the TDFS kinetics appears also to be present using MUC6 at 45 °C. Being attached to the active site by a linker shortened by one CH$_2$ unit, MUC6 probes a slightly different environment than MUC7. The contribution of the τ_3 slow component differs for the different linkers as can be seen in Table 3. At a temperature of 45 °C it is visible that the relaxation dynamics is slower for the MUC6:DhaA-H272F complex compared to MUC7:DhaA-H272F. It is tempting to view the results in light of the knowledge obtained with the AOT micelles systems and elaborate regarding hydration of these particular tunnel regions as the cause of the different Stokes shift and kinetics. However, one must keep in mind the origin of the submicrosecond kinetics in the dye:enzyme complex. Therefore, it is reasonable to suggest that the difference between the results obtained for MUC6 and MUC7 lies in the magnitude of the specific interaction between the chromophore and protein matrix. Thus, a stronger interaction could be the cause of the displayed slower kinetics for MUC6 rather than being purely a hydration effect.

TDFS Monitored by MUC6 in DbjA-H280F versus DhaA-H272F. A very different view compared to DhaA-H272F is obtained when monitoring TDFS of MUC6 in the DbjA-H280F enzyme at 10 °C (Table 3, Figure 6). This
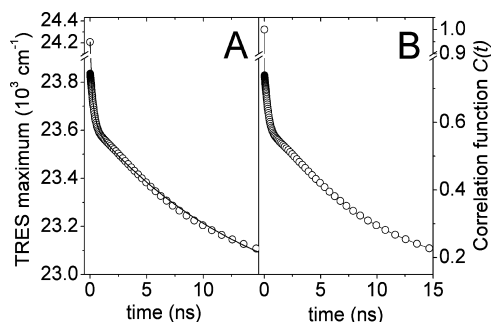

Figure 6. TDFS results obtained for MUC6:DbjA-H280F HLD, measured at 10 °C. (A) Time course of MUC6:DbjA-H280F TRES maxima, (B) correlation function $C(t)$ for MUC6:DbjA-H280F.

particular enzyme is suggested to have a significantly wider tunnel mouth than the above examined DhaA-H272F. The captured part of TDFS (75% obs, Table 3) together with the largest overall Stokes shift (1420 cm^{-1}) of all dye:enzyme complexes indicates that already at 10 °C a large part of the TDFS occurs during the nanosecond lifetime of the MUC dye. In this case the reorganization of dipole moments surrounding the MUC dye is relatively faster, and a state closer to equilibrium is reached. When comparing the different MUC6:HLD complexes at 10 °C it appears that the suggested wider tunnel mouth of DbjA-H280F makes for a weaker specific interaction between the MUC probe and the protein matrix, which we believe to be responsible for the "virtual" submicrosecond TDFS probed for DhaA-H272F.

We also find for the DbjA-H280F enzyme a different TDFS kinetics for MUC6 when compared to the one reported for the Coumarin-120 dye. The overall relaxation time τ_{SR} reported by MUC6 is significantly slower than in the case of the Coumarin-120:DbjA-H280F complex (6.7 versus 2.8 ns, respectively). This difference is however much less pronounced than for the above-described DhaA-H272F with the anticipated narrower tunnel mouth. This fact supports the hypothesis that the slow TDFS probed for DhaA-H272F is caused by a specific interaction between the MUC dye and the protein matrix.

Final Remarks on the Entire Fluorescence Data Collected for DbjA-H280F versus DhaA-H272F. Finally, the entire results obtained for DbjA-H280F and DhaA-H272F labeled with MUC variants and Coumarin-120 were compared. The results with both types of dyes are similar in a qualitative manner. The quenching data (Table 2) shows that both types of probes are more accessible to quencher molecules when attached to DbjA-H280F, indicating that it possesses a broader tunnel mouth compared to DhaA-H272F. The values of steady-state anisotropy are also in agreement for both MUC and Coumarin-120 dyes. DbjA-H280F displays lower anisotropy values, implying a higher motional freedom of the probes than in the DhaA-H272F enzymes. When considering that for DhaA-H272F at 10 °C the reorientation of the protein matrix is not complete during the nanosecond lifetime of the MUC dye we can conclude that the kinetics of the process is significantly slower in this case comparing to DbjA-H280F. Those findings

point to a lower mobility and hydration within the tunnel mouth of DhaA-H272F when compared to DbjA-H280F.

The magnitude of the differences between both HLD enzymes is, however, probe dependent. TDFS monitored with Coumarin-120 occurs on the nanosecond time scale for DbjA-H280F and DhaA-H272F. In this case the differences for both enzymes are significant and can be quantitatively expressed by the overall relaxation time τ_{SR} and overall dynamic Stokes shift $\Delta\nu$. The observation that the probed reorientation for DhaA-H272F labeled with MUC dyes is not complete within the fluorescence lifetime somewhat complicates conclusions, and the magnitude of the estimated parameters has to be analyzed with care. Nonetheless, data collected by MUC6 seems to clearly qualitatively support the conclusions drawn from the Coumarin-120 experiments. All observations here reported are consistent with the crystal structures of DbjA[30] and DhaA.[45]

■ CONCLUSIONS

In this study we designed, synthesized, and characterized a set of new fluorescence probes derived from dimethylaminonaphthalene, named MUC dyes. Measurements carried out in solvents and AOT reverse micelles proved that the fluorescence properties of the newly synthesized dye are significantly improved, specifically for their use in TDFS studies, when compared to the dye based on Coumarin-120, which had been previously used for monitoring mobility and hydration at the tunnel mouth of HLDs DbjA-H280F and DhaA-H272F. We monitored the TDFS of this particular functionally important region of DbjA-H280F and DhaA-H272F with the new MUC dye possessing two different linker lengths: MUC6 and MUC7.

In general, the overall trends in TDFS kinetics found with the new dye support those obtained with Coumarin-120, i.e., the tunnel mouth region of DhaA-H272F has a substantially slower dynamics than that of DbjA-H280F and appears to possess a lower degree of hydration.

As far as DbjA-H280F is concerned, the TDFS response of the MUC probe occurs during a nanosecond time scale but still is slower than the TDFS probed by the Coumarin-120 dye. In contrast, the reorientation kinetics in the tunnel mouth of DhaA-H272F probed by the MUC dye appears to be significantly shifted toward the longer submicrosecond domain being, therefore, out of the reach of MUC's fluorescence lifetime.

In summary, we successfully labeled specifically the tunnel mouth of the two HLDs with the MUC dyes possessing an identical linker to the one used previously with Coumarin-120. Both MUC and Coumarin-120 chromophores positioned at a similar site within the enzyme structure report qualitatively comparable information on the differences in mobility and hydration among the two examined HLD enzymes. The TDFS profile probed by the MUC dyes in DhaA-H272F's tunnel mouth completely differs from the one recorded by the Coumarin-120 dye. The findings here reported illustrate that the chemical nature of the chromophore might lead to specific interactions with the protein matrix which alter drastically the TDFS response. The narrower the tunnel mouth and the deeper the location of the MUC dye, the stronger such interaction appears to be. Nonetheless, even in such cases qualitative comparisons between carefully designed experiments might still be possible and thus provide useful information.

ASSOCIATED CONTENT

S **Supporting Information**

Details of MUC dyes synthesis, NMR spectra of MUC intermediates, photophysical characterization of MUC dyes, and "time 0 estimation" procedure. This material is available free of charge via the Internet at http://pubs.acs.org.

AUTHOR INFORMATION

Corresponding Author

*E-mail: radka@chemi.muni.cz; jan.sykora@jh-inst.cas.cz; paruch@chemi.muni.cz.

Notes

The authors declare no competing financial interest.

ACKNOWLEDGMENTS

REFERENCES

(1) Eisenmesser, E. Z.; Millet, O.; Labeikovsky, W.; Korzhnev, D. M.; Wolf-Watz, M.; Bosco, D. A.; Skalicky, J. J.; Kay, L. E.; Kern, D. Intrinsic Dynamics Of An Enzyme Underlies Catalysis. *Nature* **2005**, *438*, 117−121.

(2) Schwartz, S. D.; Schramm, V. L. Enzymatic Transition States And Dynamic Motion In Barrier Crossing. *Nat. Chem. Biol.* **2009**, *5*, 552−559.

(3) Henzler-Wildman, K.; Kern, D. Dynamic Personalities Of Proteins. *Nature* **2007**, *450*, 964−972.

(4) Bueno, M.; Temiz, N. A.; Camacho, C. J. Novel Modulation Factor Quantifies The Role Of Water Molecules In Protein Interactions. *Proteins* **2010**, *78*, 3226−3234.

(5) Privett, H. K.; Kiss, G.; Lee, T. M.; Blomberg, R.; Chica, R. A.; Thomas, L. M.; Hilvert, D.; Houk, K. N.; Mayo, S. L. Iterative Approach To Computational Enzyme Design. *Proc. Natl. Acad. Sci. U.S.A.* **2012**, *109*, 3790−3795.

(6) Koehorst, R. B. M.; Laptenok, S.; Van Oort, B.; Van Hoek, A.; Spruijt, R. B.; Van Stokkum, I. H. M.; Van Amerongen, H.; Hemminga, M. A. Profiling Of Dynamics In Protein-Lipid-Water Systems: A Time-Resolved Fluorescence Study Of A Model Membrane Protein With The Label Badan At Specific Membrane Depths. *Eur. Biophys. J. Biophys. Lett.* **2010**, *39*, 647−656.

(7) Shaw, A. K.; Sarkar, R.; Banerjee, D.; Hintschich, S.; Monkman, A.; Pal, A. K. Direct Observation Of Protein Residue Solvation Dynamics. *J. Photochem. Photobiol. A: Chem.* **2007**, *185*, 76−85.

(8) Jurkiewicz, P.; Cwiklik, L.; Jungwirth, P.; Hof, M. Lipid Hydration And Mobility: An Interplay Between Fluorescence Solvent Relaxation Experiments And Molecular Dynamics Simulations. *Biochimie* **2012**, *94*, 26−32.

(9) Bose, S.; Adhikary, R.; Mukherjee, P.; Song, X. Y.; Petrich, J. W. Considerations For The Construction Of The Solvation Correlation Function And Implications For The Interpretation Of Dielectric Relaxation In Proteins. *J. Phys. Chem. B* **2009**, *113*, 11061−11068.

(10) Jesenska, A.; Sykora, J.; Olzynska, A.; Brezovsky, J.; Zdrahal, Z.; Damborsky, J.; Hof, M. Nanosecond Time-Dependent Stokes Shift At The Tunnel Mouth Of Haloalkane Dehalogenases. *J. Am. Chem. Soc.* **2009**, *131*, 494−501.

(11) Stratt, R. M.; Maroncelli, M. Nonreactive Dynamics In Solution: The Emerging Molecular View Of Solvation Dynamics And Vibrational Relaxation. *J. Phys. Chem.* **1996**, *100*, 12981−12996.

(12) Horng, M. L.; Gardecki, J. A.; Papazyan, A.; Maroncelli, M. Subpicosecond Measurements Of Polar Solvation Dynamics - Coumarin-153 Revisited. *J. Phys. Chem.* **1995**, *99*, 17311−17337.

(13) Richert, R.; Stickel, F.; Fee, R. S.; Maroncelli, M. Solvation Dynamics And The Dielectric Response In A Glass-Forming Solvent - From Picoseconds To Seconds. *Chem. Phys. Lett.* **1994**, *229*, 302−308.

(14) Halle, B.; Nilsson, L. Does The Dynamic Stokes Shift Report On Slow Protein Hydration Dynamics? *J. Phys. Chem. B* **2009**, *113*, 8210−8213.

(15) Zhong, D. P.; Pal, S. K.; Zewail, A. H. Biological Water: A Critique. *Chem. Phys. Lett.* **2011**, *503*, 1−11.

(16) Nilsson, L.; Halle, B. Molecular Origin Of Time-Dependent Fluorescence Shifts In Proteins. *Proc. Natl. Acad. Sci. U.S.A.* **2005**, *102*, 13867−13872.

(17) Zhang, L. Y.; Yang, Y.; Kao, Y. T.; Wang, L. J.; Zhong, D. P. Protein Hydration Dynamics And Molecular Mechanism Of Coupled Water-Protein Fluctuations. *J. Am. Chem. Soc.* **2009**, *131*, 10677−10691.

(18) Li, T. P.; Hassanali, A. A. P.; Kao, Y. T.; Zhong, D. P.; Singer, S. J. Hydration Dynamics And Time Scales Of Coupled Water-Protein Fluctuations. *J. Am. Chem. Soc.* **2007**, *129*, 3376−3382.

(19) Pan, C. P.; Callis, P. R.; Barkley, M. D. Dependence Of Tryptophan Emission Wavelength On Conformation In Cyclic Hexapeptides. *J. Phys. Chem. B* **2006**, *110*, 7009−7016.

(20) Qiu, W. H.; Kao, Y. T.; Zhang, L. Y.; Yang, Y.; Wang, L. J.; Stites, W. E.; Zhong, D. P.; Zewail, A. H. Protein Surface Hydration Mapped By Site-Specific Mutations. *Proc. Natl. Acad. Sci. U.S.A.* **2006**, *103*, 13979−13984.

(21) Chang, C. W.; He, T. F.; Guo, L. J.; Stevens, J. A.; Li, T. P.; Wang, L. J.; Zhong, D. P. Mapping Solvation Dynamics At The Function Site Of Flavodoxin In Three Redox States. *J. Am. Chem. Soc.* **2010**, *132*, 12741−12747.

(22) Lampa-Pastirk, S.; Beck, W. F. Polar Solvation Dynamics In Zn(Ii)-Substituted Cytochrome C: Diffusive Sampling Of The Energy Landscape In The Hydrophobic Core And Solvent-Contact Layer. *J. Phys. Chem. B* **2004**, *108*, 16288−16294.

(23) Abbyad, P.; Shi, X.; Childs, W.; Mcananey, T. B.; Cohen, E. B.; Boxer, S. G. Measurement Of Solvation Responses At Multiple Sites In A Globular Protein. *J. Phys. Chem. B* **2007**, *111*, 8269.

(24) Guha, S.; Sahu, K.; Roy, D.; Mondal, S. K.; Roy, S.; Bhattacharyya, K. Slow Solvation Dynamics At The Active Site Of An Enzyme: Implications For Catalysis. *Biochemistry* **2005**, *44*, 8940−8947.

(25) Changenet-Barret, P.; Choma, C. T.; Gooding, E. F.; Degrado, W. F.; Hochstrasser, R. M. Ultrafast Dielectric Response Of Proteins From Dynamics Stokes Shifting Of Coumarin In Calmodulin. *J. Phys. Chem. B* **2000**, *104*, 9322−9329.

(26) Samaddar, S.; Mandal, A. K.; Mondal, S. K.; Sahu, K.; Bhattacharyya, K.; Roy, S. Solvation Dynamics Of A Protein In The Pre Molten Globule State. *J. Phys. Chem. B* **2006**, *110*, 21210−21215.

(27) Los, G. V.; Encell, L. P.; Mcdougall, M. G.; Hartzell, D. D.; Karassina, N.; Zimprich, C.; Wood, M. G.; Learish, R.; Ohane, R. F.; Urh, M.; Simpson, D.; Mendez, J.; Zimmerman, K.; Otto, P.; Vidugiris, G.; Zhu, J.; Darzins, A.; Klaubert, D. H.; Bulleit, R. F.; Wood, K. V. Hatotag: A Novel Protein Labeling Technology For Cell Imaging And Protein Analysis. *ACS Chem. Biol.* **2008**, *3*, 373−382.

(28) Koudelakova, T.; Chovancova, E.; Brezovsky, J.; Monincova, M.; Fortova, A.; Jarkovsky, J.; Damborsky, J. Substrate Specificity Of Haloalkane Dehalogenases. *Biochem. J.* **2011**, *435*, 345−354.

(29) Pavlova, M.; Klvana, M.; Prokop, Z.; Chaloupkova, R.; Banas, P.; Otyepka, M.; Wade, R. C.; Tsuda, M.; Nagata, Y.; Damborsky, J. Redesigning Dehalogenase Access Tunnels As A Strategy For Degrading An Anthropogenic Substrate. *Nat. Chem. Biol.* **2009**, *5*, 727−733.

(30) Prokop, Z.; Sato, Y.; Brezovsky, J.; Mozga, T.; Chaloupkova, R.; Koudelakova, T.; Jerabek, P.; Stepankova, V.; Natsume, R.; Van Leeuwen, J. G. E.; Janssen, D. B.; Florian, J.; Nagata, Y.; Senda, T.; Damborsky, J. Enantioselectivity Of Haloalkane Dehalogenases And

7905

dx.doi.org/10.1021/jp403708c | *J. Phys. Chem. B* 2013, 117, 7898−7906

Its Modulation By Surface Loop Engineering. *Angew. Chem., Int. Ed.* **2010**, *49*, 6111−6115.

(31) Biedermannova, L.; Prokop, Z.; Gora, A.; Chovancova, E.; Kovacs, M.; Damborsky, J.; Wade, R. C. A Single Mutation In A Tunnel To The Active Site Changes The Mechanism And Kinetics Of Product Release In Haloalkane Dehalogenase Linb. *J. Biol. Chem.* **2012**, *287*, 29062−29074.

(32) Koudeláková, T.; Chaloupková, R.; Brezovský, J.; Prokop, Z.; Pavlová, M.; Šebestová, E.; Hessler, M.; Khabiri, M.; Plevaka, M.; Kulik, D.; Kuta Smatanová, I.; Řezáčová, P.; Ettrich, R.; Bornscheuer, U. T.; Damborský, J. Engineering Protein Resistance To Organic Co-Solvent And Elevated Temperature By Access Tunnel Modification. *Angew. Chem., Int. Ed.* **2013**, Doi: 10.1002/Ange.201206708.

(33) Kulakova, A. N.; Larkin, M. J.; Kulakov, L. A. The Plasmid-Located Haloalkane Dehalogenase Gene From *Rhodococcus Rhodochrous* Ncimb 13064. *Microbiology* **1997**, *143*, 109−115.

(34) Sato, Y.; Monincova, M.; Chaloupkova, R.; Prokop, Z.; Ohtsubo, Y.; Minamisawa, K.; Tsuda, M.; Damborsky, J.; Nagata, Y. Two Rhizobial Strains, *Mesorhizobium Loti* Maff303099 And *Bradyrhizobium Japonicum* Usda110, Encode Haloalkane Dehalogenases With Novel Structures And Substrate Specificities. *Appl. Environ. Microb.* **2005**, *71*, 4372−4379.

(35) Chakrabarty, D.; Hazra, P.; Chakraborty, A.; Sarkar, N. Dynamics Of Solvation And Rotational Relaxation In Neutral Brij 35 And Brij 58 Micelles. *Chem. Phys. Lett.* **2004**, *392*, 340−347.

(36) Shirota, H.; Tamoto, Y.; Segawa, H. Dynamic Fluorescence Probing Of The Microenvironment Of Sodium Dodecyl Sulfate Micelle Solutions: Surfactant Concentration Dependence And Solvent Isotope Effect. *J. Phys. Chem. A* **2004**, *108*, 3244−3252.

(37) Sykora, J.; Kapusta, P.; Fidler, V.; Hof, M. On What Time Scale Does Solvent Relaxation In Phospholipid Bilayers Happen? *Langmuir* **2002**, *18*, 571−574.

(38) Luisi, P. L.; Straub, B. *Reverse Micelles: Biological And Technological Relevance Of Amphiphilic Structures In Apolar Media*; Plenum Press: New York, 1984.

(39) Vincent, M.; Gallay, J. Water Gradient In The Membrane Water Interface: A Time-Resolved Study Of The Series Of N-(9-Anthroyloxy) Stearic Acids Incorporated In Aot/Water/Iso-Octane Reverse Micelles. *J. Phys. Chem. B* **2012**, *116*, 1687−1699.

(40) Nagata, Y.; Hynkova, K.; Damborsky, J.; Takagi, M. Construction And Characterization Of Histidine-Tagged Haloalkane Dehalogenase (Linb) Of A New Substrate Class From A Gamma-Hexachlorocyclohexane-Degrading Bacterium, Sphingomonas Paucimobilis Ut26. *Protein Expression Purif,* **1999**, *17*, 299−304.

(41) Chattopadhyay, A.; Mukherjee, S.; Raghuraman, H. Reverse Micellar Organization And Dynamics: A Wavelength-Selective Fluorescence Approach. *J. Phys. Chem. B* **2002**, *106*, 13002−13009.

(42) Moilanen, D. E.; Fenn, E. E.; Wong, D.; Fayer, M. D. Water Dynamics In Large And Small Reverse Micelles: From Two Ensembles To Collective Behavior. *J. Chem. Phys.* **2009**, *131*.

(43) Douhal, A.; Angulo, G.; Gil, M.; Organero, J. A.; Sanz, M.; Tormo, L. Observation Of Three Behaviors In Confined Liquid Water Within A Nanopool Hosting Proton-Transfer Reactions. *J. Phys. Chem. B* **2007**, *111*, 5487−5493.

(44) Pal, H.; Nad, S.; Kumbhakar, M. Photophysical Properties Of Coumarin-120: Unusual Behavior In Nonpolar Solvents. *J. Chem. Phys.* **2003**, *119*, 443−452.

(45) Newman, J.; Peat, T. S.; Richard, R.; Kan, L.; Swanson, P. E.; Affholter, J. A.; Holmes, I. H.; Schindler, J. F.; Unkefer, C. J.; Terwilliger, T. C. Haloalkane Dehalogenase: Structure Of A *Rhodococcus* Enzyme. *Biochemistry* **1999**, *38*, 16105−16114.

(46) Fee, R. S.; Maroncelli, M. Estimating The Time-Zero Spectrum In Time-Resolved Emission Measurements Of Solvation Dynamics. *Chem. Phys.* **1994**, *183*, 235−247.

(47) Abbyad, P.; Childs, W.; Shi, X. H.; Boxer, S. G. Dynamic Stokes Shift In Green Fluorescent Protein Variants. *Proc. Natl. Acad. Sci. U.S.A.* **2007**, *104*, 20189−20194.

(48) Vincent, M.; Gilles, A. M.; De La Sierra, I. M. L.; Briozzo, P.; Barzu, O.; Gallay, J. Nanosecond Fluorescence Dynamic Stokes Shift Of Tryptophan In A Protein Matrix. *J. Phys. Chem. B* **2000**, *104*, 11286−11295.

(49) Pierce, D. W.; Boxer, S. G. Dielectric-Relaxation In A Protein Matrix. *J. Phys. Chem.* **1992**, *96*, 5560−5566.

(50) Mitra, R. K.; Sinha, S. S.; Pal, S. K. Temperature-Dependent Hydration At Micellar Surface: Activation Energy Barrier Crossing Model Revisited. *J. Phys. Chem. B* **2007**, *111*, 7577−7583.

(51) Beranova, L.; Humpolickova, J.; Sykora, J.; Benda, A.; Cwiklik, L.; Jurkiewicz, P.; Grobner, G.; Hof, M. Effect Of Heavy Water On Phospholipid Membranes: Experimental Confirmation Of Molecular Dynamics Simulations. *Phys. Chem. Chem. Phys.* **2012**, *14*, 14516−14522.